ESTIMATES OF DIRECTIONAL SPECTRA FROM THE SURFACE ACOUSTIC SHEAR SENSOR (SASS)

Markku J. Santala and Albert J. Williams III

Woods Hole Oceanographic Institution
Woods Hole, Massachusetts

Abstract

The SASS (Surface Acoustic Shear Sensor) is a newly developed instrument platform designed to study upper ocean mixing processes. It consists of an array of six vector-measuring acoustic velocity sensors and a gyro stabilized motion sensing package mounted onto a moored surface-following float. Because SASS is instrumented with a motion sensing package, we are provided with an opportunity to discuss the effects of sensor motion on the estimation of directional wave spectra.

Introduction

Within this paper we describe the Surface Acoustic Shear Sensor (SASS). The SASS is an instrument which was initially developed to examine the wind-induced shear in the upper 6m of the ocean. The SASS was designed to be a surface-following float because it is believed that the near-surface shear current is roughly parallel to the instantaneous surface of the fluid and that the effect of long waves is just to advect the shear current up-and-down[1].

However, a current meter which moves coherently with wave motions is biased by rectification of the orbital velocities of waves[2]. To allow for compensation of this effect, SASS was designed with a motion sensing package that measures all six degrees of freedom of motion. Correction for this effect is a subtle issue that will be discussed elsewhere[3].

Here we examine the effect of sensor motion on estimates of directional spectra. It is found that the traditional assumption that the sensor is fixed in position is extremely good in the energetic part of the spectrum. This motion effect will probably only be important when investigators seek to evaluate the calibration of their instruments or for other specialized purposes.

Design of SASS

To measure velocities with respect to the surface a buoy needs a large waterplane area. As is noted by Collar *et al*[4], velocity sensors beneath discus shaped buoys become trapped in the boundary layer beneath the buoy and give unreliable results. For this reason the buoyancy elements of the SASS were divided into three pods as is shown in Figure 1. Each float is $0.84m$ high but with the combination of pods giving a total waterplane area of $2.0m^2$ only $0.28m$ of draft is necessary to float the $5.5kN$ (wet)buoy. This leaves $11kN$ of excess buoyancy. This shallowness of draft and distance of seperation (in plan view SASS is an equilateral triangle $3.7m$ on a side) made for minimal flow disturbance. A truss, constructed of $2inch$-OD aluminum tubing, connects the buoyancy elements and provides a rigid structure to which the current meter array could be attached and through which mooring forces could be transmitted.

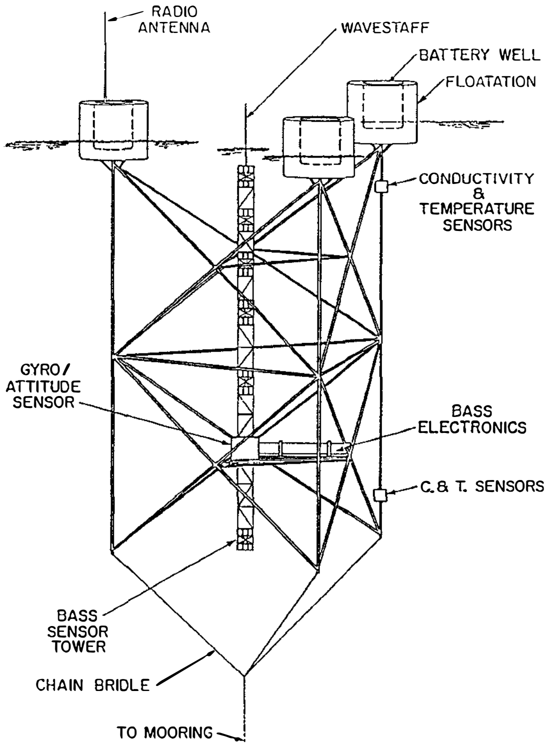

Figure 1. The SASS platform. The six velocity sensors are fixed in the center of the rigid support truss. The truss is $3.7m$ on each side and $6.0m$ high. The floatation pods add $0.84m$ to the overall height.

Velocities relative to the instrument are measured with the BASS three-axis acoustic current meter[5]. Sensing volumes were located at each of the six following depths (in cm): 111, 166, 251, 311, 391 and 585. With a sampling volume $O(15cm)$ in length, and a near-perfect cosine response, this current meter allows us to obtain an accurate time history of the fluid velocities in an instrument based frame of reference. A two axis gyroscope, manufactured by Colnbrook, provided a stailized platform on which accelerometers were mounted to measure translational motions. Two capacitive type potentiometers measured the tilt of the buoy by referencing the gyro platform. The yaw rotations were measured by a compass inside the BASS pressure case. Having measured all six degress of freedom of the instrument's motion allows us to not only rotate the relative velocities into an inertial frame of reference, but also allows us to add in the instrument velocity. Thus, a time series of the fluid velocity (at the point of the sensor) may be obtained. In order to measure how well SASS follows the water's surface, a wavstaff was mounted directly above the sensor column.

Measuring the stability of the water column is important for a shear sensor. The thermal gradient was measured by mounting small metal-clad thermistors directly adjacent to each BASS sensing volume. Though the small size of these sensors causes little flow disturbance they do not provide an extremely accurate absolute measurement of temperature. To this end, Sea-Bird thermistors were mounted at the same elevation as the top and bottom metal-clad thermistors (but far off to the side as these sensors are quite large). Each Sea-Bird thermistor was accompanied by a conductivity sensor.

The SASS was operated so that all channels were sampled at 4Hz. Each record was 89 bytes long so that in the typical hour long files it was necessary to store 1.25 Mbytes of data. Data could be stored in one of two ways; it could be transmitted to ship or shore via Clegg FM transciever or it could be stored to an optical disk which was housed inside one of the battery wells. When not transmitting data the transciever was in a listening mode. A menu of 12 command options controlling SASS instrumentation could be selected by transmitting a DTMF signal to SASS. This signal was decoded and interpreted by a Tattletale IV computer which turned sensors on and off by a series of FET switches attached to its I/O lines.

The radio transmitter requires 24 Watts of power and the gyro 18 Watts. If all data were to be transmitted the rechargeable batteries provide enough power to recover 46 hours of data. Recording data to optical disk provides hard-wired reliability to the data recovery but at the cost that the disk requires 20 percent more power than the radio.

Transformation of coordinates

The goal is to obtain the instantaneous velocity of the fluid, $\mathbf{V}(\mathbf{x},t)$, at the point of the sensor, $\mathbf{X}(t)$, as a function of time in an inertial set of coordinates.

$$\mathbf{V}^{(i)}(\mathbf{X}(t);t) = \mathbf{V}_S^{(i)}(t) + \mathbf{V}_{rel}^{(i)}(\mathbf{X}(t);t) \qquad (1)$$

$\mathbf{V}_{rel}^{(i)}$ is the velocity of the fluid relative to the i^{th}–sensor and $\mathbf{V}_S^{(i)}$ is the velocity of the i^{th}-sensor. $\mathbf{V}_{rel}^{(i)}$ is found by transforming the velocity measured in instrument coordinates via the rotational-translation matrix. The rotational-translation matrix is a function of the pitch, roll and yaw angles of the buoy.

Accelerometers are fixed to the stabilized platform of the gyro and thus only translate and yaw with respect to inertial coordinates. Accelerometer outputs are rotated into an inertial frame and then integrated once to find the linear velocity of the SASS's defined coordinate origin. The velocity of each sensor is composed of this linear velocity and a rotational velocity component. The translational velocity of the i^{th}– sensor is

$$\mathbf{V}_S^{(i)} = \frac{d\mathbf{R}_\bullet}{dt} + \omega \times \mathbf{r}^{[i]} \qquad (2)$$

where ω is the angular velocity of the body, which may be found from the pitch, roll and yaw angles and their derivatives. The $\mathbf{r}^{[i]}$ are distance vectors originating from the SASS's defined origin and terminating at the i^{th}–sensor.

Estimation of directional spectra

In interpreting shear current profiles from SASS it will be useful to know how energetic waves were and from which direction they were travelling during a sampling event. The traditional way of estimating directional spectra from a surface following float is to use the pitching and rolling motions of the buoy as was done by Longuet-Higgins *et al*[6]. With SASS we find this is not the best way to proceed.

With a horizontal length scale of $3.7m$, it would not be reasonable to expect that the buoy could accurately follow waves considerably longer than twice this length. Further, pitch and roll estimates are heavily dependent on the transfer function of a buoy. SASS is a complex moored structure and prediction of a transfer function would be extremely difficult. Of course, with all the relative velocities and sensor velocities being measured a transfer function could be derived. Rather than take this circuitous path we can just use the field velocities of the fluid, $\mathbf{V}^{(i)}(\mathbf{x},t)$, instead of the heave, pitch and roll. Barrick *et al*[7] have demonstrated that not only will errors in transfer function estimation degrade spectral estimates but so too will the nonlinearities of the wavefield.

In correlating the components of $\mathbf{V}$ to estimate directional spectra we avoid both of the aforementioned problems. The motion of SASS is measured and thus there is no need to estimate the transfer function. The Stokes' expansion of waves predicts that nonlinearities are two orders of magnitude smaller (when scaled by waveslope Ak) in the velocity field than in the height/slope field[8].

One problem that does remain is that SASS is a moving sensor. The pitch and roll theory assumes measurements are made at a fixed point, $\mathbf{X}_o$,

$$\tilde{\mathbf{V}}(\mathbf{X}(t);t) \approx \mathbf{V}(\mathbf{X}_o;t) \qquad (3)$$

(tilde denotes measured velocity). Using potential theory expressions for the orbital velocities we see that to $O(Ak\mathbf{V})$

$$\begin{aligned}\tilde{\mathbf{V}}(t) &= \mathbf{V}(\mathbf{X}_o;t) + \left[jk(t) * \int_\theta \cos\theta \mathbf{V}(\theta,t)d\theta\right]\cdot x(t) \qquad (4)\\ &+ \left[jk(t) * \int_\theta \sin\theta \mathbf{V}(\theta,t)d\theta\right]\cdot y(t) + [k(t) * \mathbf{V}(t)]\cdot z(t)\end{aligned}$$

with $j = \sqrt{-1}$, k being the wavenumber, and θ being the angle in the horizontal $(x-y)$ plane (we take z to be upwards). $\tilde{V}_1, \tilde{V}_2, \tilde{V}_3$ are the field velocities measured in the inertial coordinates x, y, z. The $*$ indicates convolution. The cross-spectra $S_{V_iV_j} = C_{V_iV_j} - jQ_{V_iV_j}$ are needed to estimate the directional spectra of the wavefield. If we denote radian frequency by σ, then we may express that the spectrum measured by the moving sensor will equal the spectrum at the mean location plus a "modulation spectrum" as

$$S_{\tilde{V}_i\tilde{V}_j}(\sigma) = S_{V_iV_j}(\sigma) + S_{MOD_{ij}}(\sigma) \tag{5}$$

From (4) we find $S_{MOD_{ij}}$ to be

$$\begin{aligned} S_{MOD_{ij}} &= \left\{k^2(\sigma)S_{V_iV_j}(\sigma)\int_\theta \cos^2\theta D(\sigma,\theta)d\theta\right\} * S_{XX}(\sigma) \\ &+ \left\{k^2(\sigma)S_{V_iV_j}(\sigma)\int_\theta \sin^2\theta D(\sigma,\theta)d\theta\right\} * S_{YY}(\sigma) \\ &+ \left\{k^2(\sigma)S_{V_iV_j}(\sigma)\right\} * S_{ZZ}(\sigma) \qquad (6) \\ &+ \left\{k^2(\sigma)S_{V_iV_j}(\sigma)\int_\theta \cos\theta\sin\theta D(\sigma,\theta)d\theta\right\} * 2\Re(S_{XY}(\sigma)) \\ &+ \left\{k^2(\sigma)S_{V_iV_j}(\sigma)\int_\theta \cos\theta D(\sigma,\theta)d\theta\right\} * 2\Im(S_{ZX}(\sigma)) \\ &+ \left\{k^2(\sigma)S_{V_iV_j}(\sigma)\int_\theta \sin\theta D(\sigma,\theta)d\theta\right\} * 2\Im(S_{ZY}(\sigma)) \end{aligned}$$

The wave spreading function, $D(\sigma,\theta)$, is normalized so that $\int_\theta D(\sigma,\theta)d\theta = 1$. $\Re$ and $\Im$ indicate where the real or imaginary part of the cross-spectrum is to be taken. Let's consider the form of equation (6). Each term is the cross-spectrm of the velocities to be estimated, times the wavenumber squared, convolved with a sensor displacement spectrum. Sensor motions should be the same order of magnitude as the wave orbital excursions. In this case it is clear that $S_{MOD} \sim (Ak)^2 S_{V_iV_j}$. Because the modulated energy is scaled by the waveslope squared this effect is usually ignored. However, since the spectra are convolved, we expect that the peaks in the modulation spectrum will be located at the sums and differences of the peaks of the fluid velocity spectra and motion spectra. With wave spectra typically being narrowband, this allows for the possibility that the energy is modulated into band where $k^2(\sigma_{peak_V})S_{V_iV_j}(\sigma_{peak_V})S_{X_aX_b}(\sigma_{peak_X})$ is non-negligible.

Example

We demonstrate these ideas with a data file obtained by the SASS. The SASS has been deployed twice as part of the Shelf MIxed Layer Experiment (SMILE)[9]. The data shown here was recorded on December 12, 1988 beginning at 10:46*am*. The SASS was at this time moored at 38°-38.9'N 123° -29.3'W, about 5*km* off the coast of Northern California in a water depth of 90*m*.

modulation effect

Figure 2 shows the co-spectrum of vertical velocity, $C_{\tilde{V}_3\tilde{V}_3}$, as measured by the uppermost BASS pod. The position of the pod was nearly a constant distance below the instantaneous surface; the *rms* wave elevation was 58*cm*, while the *rms* wavestaff signal (indicating relative motion between the buoy's waterline and the instantaneous surface elevation) was only 1.7*cm*. As is evidenced in the figure, there was a strong swell peak and a small wind wave peak. The wind waves were, at this point, dying down. The windspeed, at the time of data recording, was down to an average speed of 2.1m/s from the 4.1m/s average speed of the previous night.

Also plotted on Figure 2 is the estimate of the modulated energy in the co-spectrum. As is seen, this energy is for the most part negligible, especially near the peak frequencies. However, as the expanded view of Figure 3 shows, the peaks in $C_{MOD_{33}}$ reach their maxima in the spectral gaps of $C_{\tilde{V}_3\tilde{V}_3}$. So, in the 0.23Hz region $C_{MOD_{33}}$ is approximately 15% of the estimated co-spectrum, and in the 0.40Hz region $C_{MOD_{33}}$ is approximately 40% of the estimated co-spectrum. Estimates shown represent 21*min*-20*sec* of data (5120 samples). The data was subdivided into blocks of length 256 points with 50% overlap. The resulting 39 blocks of data were windowed with a cosine-squared taper and then Fourier transformed and averaged to obtain a spectral estimate.

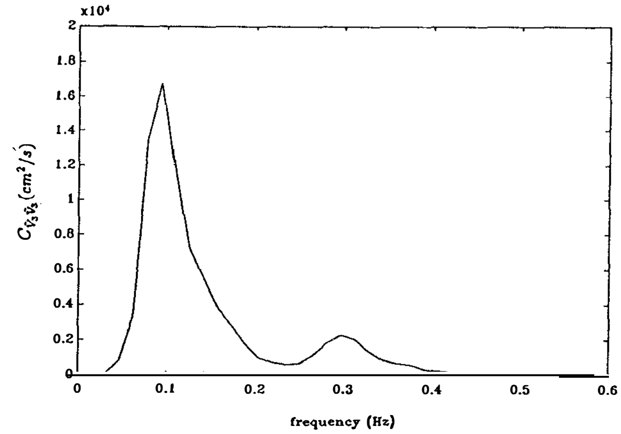

Figure 2. Co-spectrum of vertical velocity of fluid as measured by top sensor; $C_{\tilde{V}_3\tilde{V}_3}$ —. Error in $C_{V_3V_3}$ due to motion; $C_{MOD_{33}}$ ···.

To estimate the modulation co-spectrum one should know the true co-spectrum $S_{V_3V_3}$. Since this is not available, $C_{MOD_{33}}$ was estimated by assuming that $S_{V_3V_3} \approx S_{\tilde{V}_3\tilde{V}_3}$; this estimate gives the upper bound estimate of Figure 3. From this first estimate it is clear that a large fraction of the energy above 0.4Hz is error energy from $C_{MOD_{33}}$. Therefore a second estimate was made where $S_{\tilde{V}_3\tilde{V}_3}$ was lowpass filtered with a cutoff at 0.4Hz. This second estimate is the lower bound curve of Figure 3. We have not yet considered the efficacy of any iterative methods to obtain a precise estimate of the modulation.

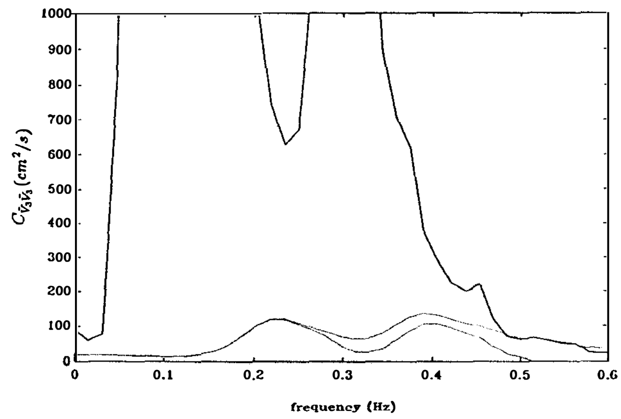

Figure 3. Same plot as Figure 2 with expanded vertical scale. $C_{\tilde{V}_3\tilde{V}_3}$ —. Error in $C_{V_3V_3}$ due to motion; $C_{MOD_{33}}$ ···.

Errors due to nonlinearities in the wavefield will be even smaller than those due to modulation. In the velocity field the highest order correction to the linearized velocity is $O((Ak)^3\mathbf{V})$ and thus the wavefield nonlinearity may bias our spectral estimates by $O((Ak)^6 S_{V_iV_j})$, as opposed to the $O((Ak)^2 S_{V_iV_j})$ effect of modulation.

One measure of how well the energy in the orbital velocities is measured is to compare the energy in the horizontal and vertical components of wave velocity[7]. Ideally, the ratio u below, is equal to unity

$$u = \frac{(C_{V_1V_1} + C_{V_2V_2})}{C_{V_3V_3}} \stackrel{?}{=} 1 \qquad (7)$$

The measured co-spectra will not satisfy this relation exactly. The ratio u is plotted from our sample SASS file in Figure 4. Note that between the frequencies of 0.05Hz to 0.45Hz the maximal deviations of u from unity occur at the peak of the modulation spectra, 0.22Hz and 0.40Hz.

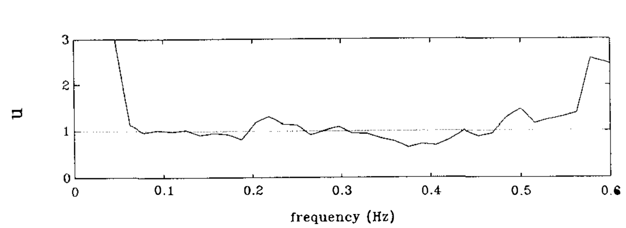

Figure 4. The ratio $u = (C_{\tilde{V}_1\tilde{V}_1} + C_{\tilde{V}_2\tilde{V}_2})/C_{\tilde{V}_3\tilde{V}_3}$, as measured by the uppermost sensing volume.

below the spectral peak

Consider typical accelerations of the buoy (relative motion between the uppermost sensing volume and the fluid, $\mathbf{V}_{rel}$, was small compared to the motion of the sensor, $\mathbf{V}_S$, so that for estimates in this section we use $\mathbf{V}$ and $\mathbf{V}_S$ interchangeably); the *rms* surface elevation was $58cm$, the peak frequency was 0.1Hz, so that the typical accelerations of the buoy may be approximated as $\eta_{rms}\sigma_{peak}^2 = 20cm/s^2 = 0.02g$ (where g is the acceleration due to gravity). This means that when there is a small error in the stabilization of the gyro platform the errors of the apparent acceleration will be much greater due to cross-sensitivity to the gravity vector than to actual buoy accelerations. In this case, if there is a small error angle, $\varepsilon(t)$, the error in the horizontal acceleration of the buoy, $\ddot{X}_{err}$, and the vertical acceleration of the buoy, $\ddot{Z}_{err}$, may be approximated soley as a function of g and $\varepsilon(t)$ as:

$$\begin{aligned} \ddot{X}_{err} &\approx g\sin\varepsilon(t) \approx g\varepsilon(t) \\ \ddot{Z}_{err} &\approx g\left(1 - \cos\varepsilon(t)\right) \approx g\left(\frac{\varepsilon^2(t)}{2!}\right) \end{aligned} \qquad (8)$$

The ratio of errors in the velocity spectra of motion is therefore

$$\frac{S_{\dot{X}_{err}\dot{X}_{err}}}{S_{\dot{Z}_{err}\dot{Z}_{err}}} \sim \frac{4}{|\varepsilon(\sigma)|^2} \qquad (9)$$

Notice that as the error angle $\varepsilon(\sigma)$ becomes small, the ratio of $S_{\dot{X}_{err}\dot{X}_{err}}$ to $S_{\dot{Z}_{err}\dot{Z}_{err}}$ becomes larger. However, as $\varepsilon(\sigma)$ becomes very small this error would be masked by other errors.

If we look at the energy in the Fourier coefficient at the three lowest non-zero frequency bins (central frequency is 0.03125Hz) we find the energy ratio u to be 7.7. The sum $C_{11} + C_{22} = 66\left(\frac{cm}{s}\right)^2$ and $C_{33} = 8.6\left(\frac{cm}{s}\right)^2$. Approximating the low frequency error of the gyro as a pure sinusoid at frequency 0.03125Hz with an energy equal to the eccentricity in the ratio u, $57\left(\frac{cm}{s}\right)^2$, we can estimate the magnitude of the error in stabilization from

$$S_{\dot{X}_{err}\dot{X}_{err}} = \frac{g\,|\varepsilon(\sigma_o)|^2}{\sigma_o^2} \qquad (10)$$

and find that $|\varepsilon| \approx 0.00151rad$ (00°-$05'$-$11''$).

An error of such magnitude is certainly not unexpected. The gyro maintains its alignment with the local gravity vector by averaging the output of spirit-level mercury switches which allow an electrical current to pass to solenoids which slowly torque the stabilized platform. However, the mean stabilization of the mercury switches is only accurate to within 0.3°. The enormous angular momentum of the gyro, spinning at $10,000rpm$, causes the error angle to rapidly decrease with increasing frequency. It does not seem unreasonable that at frequencies in the range of 0.03Hz that there be an error angle of $5'$.

The anisotropy of the cospectra at low frequency is well explained by the "error angle argument". Previous authors[7] have attempted to explain this anomolous behaviour of u at low frequency by the presence of small amounts of wave energy at frequencies below the spectral peak. Since the SASS was moored in $90m$ of water, very low frequency waves will no longer have circular orbital trajectories but will have more energy in the horizontal excursion than in the vertical. So, if the SASS were measuring waves at extremely low frequency one would *expect* the ratio u to increase with decreasing frequency. For intermediate depth the theoretical value of u is given by

$$u = \frac{C_{V_1V_1} + C_{V_2V_2}}{C_{V_3V_3}} = \left(\frac{1}{\tanh k(z+h)}\right)^2 \qquad (11)$$

where h is the water depth. For the case under consideration, to obtain a u of 7 requires waves with a wavenumber $k = 0.00447m^{-1}$. Such a wave has a frequency of 0.020Hz. Beyond the fact that u reaches 7 at a higher frequency than 0.020Hz; if a wave of frequency 0.020Hz were to contribute energy of $66(\frac{cm}{s})^2$ it would have to have an *rms* amplitude $O(4m)$. Considering the above, it seems that for the SASS, most of the deviation of u for unity at low frequency is due to imperfect gyro stabilization.

Conclusions

The SASS, an instrument developed to measure the shear current profile in the upper $6m$ of the ocean, is capable of measuring the directional spectra of waves from estimates of the orbital velocities. Unlike traditional pitch and roll buoys, which depend on estimates of a transfer function, the SASS measures all velocities directly. Further, because SASS makes estimates from the velocity field rather than the height/slope field, the estimates are probably less sensitive to wavefield nonlinearities.

Motion of the buoy was seen to cause a modulation error in the spectral estimates. This error is quite small and will not effect estimation of the energetic portion of the spectrum. However, having brought this issue to light, anomolous behaviour in frequency bands of low energy can be explained that might have otherwise been attributed to poor calibration, processing error, or even an unknown physical process. For the SASS, the estimates of spectral energy degrade at frequencies $O(0.03\text{Hz})$ and lower; most probably due to small angular error in stabilization of the gyro platform.

We close by showing the estimate of the directional wave spectrum for the data file we considered throughout the paper (Figure 5). The maximum entropy method[10] was used to estimate the directional dependence.

acknowledgements

Assisting in the preparation and deployment of SASS were C.V.R. Dunn, E.T. Montgomery and E.A. Terray. This work was funded by NSF grant OCE-87-16937. This paper is Woods Hole Oceanographic Institution contribution 7434.

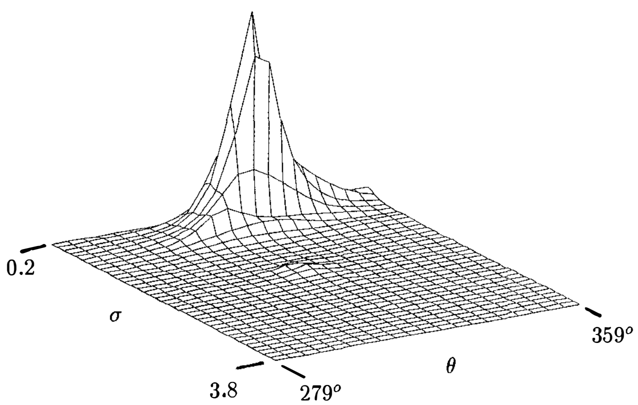

Figure 5. The directional wave spectrum derived by applying the maximum entropy method to the co- and quad-spectra of field velocity components, **V**, at the uppermost sensing volume. Waveheight was estimated from potential theory relations between velocity and waveheight. The integrated energy under the spectrum is $3360cm^2$ (directionally, magnetic north = $0°$).

References

1. CSANADY, G.T. (1984) The free surface turbulent shear layer. *Journal of Physical Oceanography*, **14**, 402-411.

2. POLLARD, R.T. (1973) Interpretation of near-surface current meter observations. *Deep-Sea Research*, **20**, 261-268.

3. SANTALA, M.J. and E.T. TERRAY (1990) A technique for making unbiased estimates of current from a wave-follower. In preperation.

4. COLLAR, P.G., R.M. CARSON and G. GRIFFITHS (1983) Measurement of near-surface current from a moored wave-slpoe follower. *Deep-Sea Research*, **30**, 63-75.

5. WILLIAMS, A.J. 3rd, J.S. TOCHKO, R.L. KOEHLER, W.D. GRANT, T.F. GROSS, and C.V.R. DUNN (1987) Measurement of turbulence in the oceanic bottom boundary layer with an acoustic current meter array. *J. Atmos. and Oceanic Tech.* **4(2)** 312-327.

6. LONGUET-HIGGINS, M.S., D.E. CARTWRIGHT and N.D. SMITH (1963) Observations of the directional spectrum of sea waves using the motions of floating buoy. *Ocean Wave Spectra*, Prentice-Hall, 111-136.

7. BARRICK, D.E., B.J. LIPA and K.E. STEELE (1989) Comments on "Theory and application of calibration techniques for an NDBC directional wave measurements buoy" : nonlinear effects. *IEEE J. Oceanic Eng.* **14(3)** 268-272.

8. WEHAUSEN, J.V. and E.V. LAITONE (1960) Surface Waves. In *Encyclopedia of Physics*, vol. 9. Berlin-Göttingen-Heidelberg : Springer-Verlag.

9. MONTGOMERY, E.T. and M.J. SANTALA (1989) The surface acoustic shear sensor (SASS) as used during the Shelf Mixed Layer Experiment. *Woods Hole Oceanog. Inst. Tech. Rept. WHOI-89-34.*

10. LYGRE, A. and H.E. KROGSTAD (1986) Maximum entropy estimation of the directional distribution in ocean wave spectra. *Journal of Physical Oceanography*, **16** 2052-2060.